

# SYNTHESIS AND OPTICAL CHARACTERIZATION OF PYROELECTRIC NANOPOWDERS BASED ON PZT (95/5)

E. PAKIZEH, S. M. HOSSEINI\*, A. KOMPANY  
and M. GHASEMIFARD

*Department of Physics (Materials and Electroceramics Laboratory)  
Ferdowsi University of Mashhad, Iran  
\*sma\_hosseini@yahoo.com*

Revised 15 January 2010

$\text{Pb}(\text{Zr}_{1-x}\text{Ti}_x)\text{O}_3$  ( $x = 0.05$ ) with pyroelectric properties have been synthesized by sol–gel technique at low temperatures. XRD results indicate that the powder has perovskite structure without secondary phases and the average of particle size was estimated to be about 40 nm in diameters. The optical constants such as refractive index,  $n$ , extinction coefficient,  $k$ , and the dielectric function of PZT nanopowders have been investigated by Fourier transmittance infrared (FTIR) spectrum and Kramers–Kronig (KK) analysis program. The use of the KK method to analyze the normal incidence infrared (IR) reflectance spectra with a single resonance has also been described. The results indicated that the optical constant increases slowly as temperature of calcinations increases.

*Keywords:* PZT (95/5); sol–gel processes; nanoparticles; Kramers–Kronig; optical properties.

## 1. Introduction

Lead zirconate titanate  $\text{Pb}(\text{Zr}_{1-x}\text{Ti}_x)\text{O}_3$  or (PZT) for  $x = 0.01$ – $0.07$  ceramics have outstanding pyroelectric and ferroelectric properties. It is used broadly in devices such as pyroelectric infrared (IR) for IR detection, spectroscopy and imaging.<sup>1,2</sup> In general, this ceramic is processed by the traditional solid state reaction, but there are undesirable features such as non-stoichiometry due to loss of Pb, compositional fluctuation and poor microstructure because of the high temperature processes.<sup>3,4</sup> Therefore, it is necessary to process PZT ceramic at a temperature as low as possible.

Low firing temperature processing in ceramic fabrication demands fine precursor powders of high homogeneity of components mixing. Nanosized

PZT precursor powder fabrication is of a special interest to sinter fine-grained piezo ceramics without ferroelectric property degradation. Chemical methods such as coprecipitation,<sup>5,6</sup> hydrothermal reaction<sup>7,8</sup> and gel-combustion<sup>9–12</sup> processes are employed nowadays to synthesis the PZT nanopowders. Many sol–gel methods make use of alkoxides as raw materials, and organic materials as solvents. On the other hand, due to the high electropositive nature elements of transition metals, adding water or alcohols to these elements quickly form hydrated oxides or alkoxides.<sup>10</sup> In addition, when alkoxides of Ti and Zr are added into a solution to form a sol or a gel, precipitates are often formed. Therefore, PZT sol must be prepared in an isolated dry condition or even in an atmosphere of dry argon or nitrogen gas.<sup>11</sup>

\*Corresponding author.

For the present work, pyroelectric nanopowders base on PZT (95/5) were prepared in air at low temperature by using the sol-gel route but with lead nitrate, zirconium nitrate and water as the raw material and primary solvent of the precursors, respectively. Though there are number of papers already published on the synthesis of PZT nanopowders, the optical properties of PZT (95/5) nanopowders have rarely been studied. Moreover, the optical characterization gives some information about structural and the optical properties of the nanopowders. For example, FTIR spectra give information on the chemical bonds and the molecular structures. From the imaginary part of dielectric function, the energy band transitions can be evaluated.

However, in this paper, the optical properties are discussed and some optical constants of synthesized PZT ceramic nanopowders have been evaluated from Kramers-Kronig analysis using FTIR spectra data. The synthetic process employed in the present investigation is easily controllable and convenient in comparison with the other methods.

## 2. Experimental

The raw materials used in this study were lead nitrate  $[\text{Pb}(\text{NO}_3)_2]$ , zirconium nitrate hydrate  $[\text{ZrO}(\text{NO}_3)_2, x\text{H}_2\text{O}]$  and titanium isopropoxide

$\text{Ti}[\text{OCH}(\text{CH}_3)_2]_4$ . Aqueous solutions of each single cation were prepared by dissolving lead nitrate and zirconyl nitrate in distilled water. For preparation of  $\text{Ti}^{+4}$ , we dissolved titanium isopropoxide in the mixture of nitric acid, citric acid and hydrogen peroxide. The PZT precursor sol was prepared by mixing the solutions of lead zirconium and titanium together. The flow diagram of the nanopowder processing methods employed in this study is shown in Fig. 1.

The PZT sol was added to the aqueous solution of citric acid under continuous stirring at temperature of  $65^\circ\text{C}$ , and the pH of the sol is maintained at 7 by adding ammonium hydroxide. The gel was prepared by heating the sol at a temperature of about  $85^\circ\text{C}$ . The resultant nanopowders were calcinated at different temperatures to obtain the desired single-phase nanopowders.

## 3. Characteristic of Nanopowders

The phase formation and orientation of PZT nanopowders were investigated using X-ray diffraction analysis in the range ( $5\text{--}60^\circ\text{C}$ .) with  $\text{CuK}\alpha$  radiation. Fourier transform infrared spectroscopy (FTIR) was used to monitor the bond between elements in the PZT nanopowders and optical properties have been investigated in the wavenumber range  $400\text{--}4000\text{ cm}^{-1}$ .

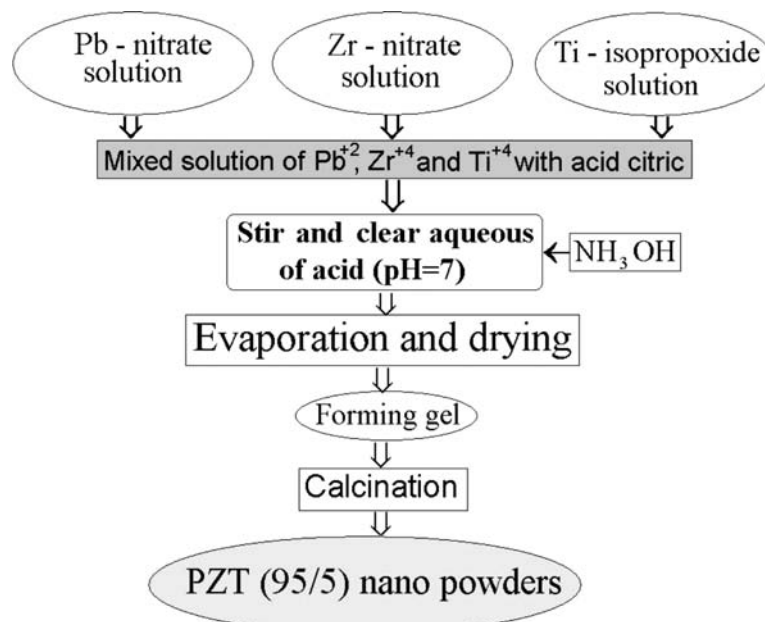


Fig. 1. Flow diagram for PZT nanopowders preparation procedure.

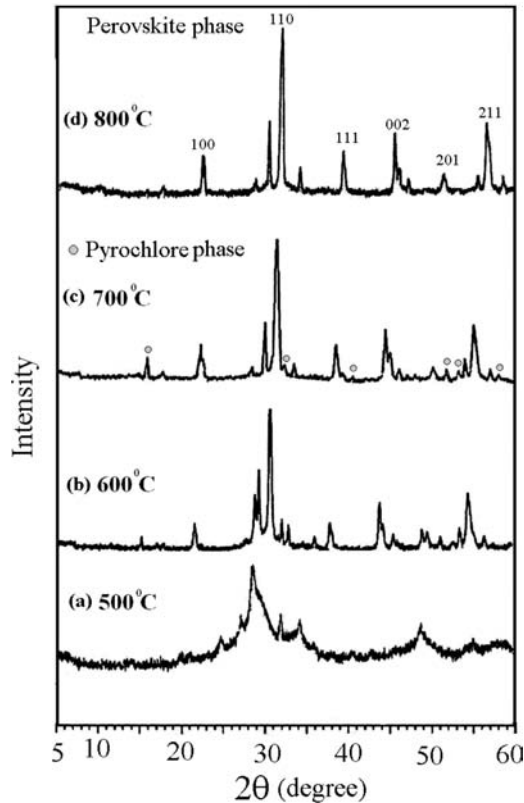


Fig. 2. XRD spectra of samples of the PZT nanopowders calcinated at different temperatures. (a) 500°C, (b) 600°C, (c) 700°C and (d) 800°C.

### 3.1. Phase analysis

X-ray diffraction patterns of pyroelectric nanopowders (heating rate: 5°C/min from room temperature to various temperatures ranging from 500°C to 800°C for 2 h) are shown in Fig. 2.

At a temperature of 800°C, the orthorhombic phase can be identified from this figure. The XRD results also reveal the coexistence of a perovskite-type phase and a pyrochlore phase for the sol-gel method in all temperatures. Increasing calcination temperatures eliminate gradually the pyrochlore phase but increase the amount and degree of crystallization of the perovskite phase. The results are consistent with previously reported observations for PZT with the same nominal composition prepared

by the sol-gel technique.<sup>13</sup> The lattice constants  $a$ ,  $b$  and  $c$  and the system structure of PZT calcinated at different temperatures were evaluated and are given in Table 1.

The crystalline size of the nanopowders has been determined by means of the X-ray line broadening method using the Scherrer equation:  $D = k\lambda / (B \cos \theta)$ . Where  $D$  is crystallite size,  $\lambda$  is the wavelength of radiation (1.54066 Å (Angstrom) for  $\text{CuK}\alpha$ ),  $k$  is a constant equal to unity,  $B$  is the corrected peak width at half maximum intensity and  $\theta$  is the peak position (30.5° used for all lines). The crystalline sizes of powders calcinated at different temperatures are summarized in Table 2.

The crystalline size of PZT powder increases, as calcinated temperature goes higher, the mean crystalline size was found to be about 40 nm for the samples.

These results are consistent with the reported data of Linardos *et al.*<sup>14</sup> They have employed two different sol-gel routes to synthesize PZT (95/5) powder. Their results indicated that both routes gave similar primary particle sizes in the range of 30–70 nm.

### 3.2. FTIR Spectrum

FTIR spectroscopy was used to investigate the vibration spectrum in the range of 400–4000  $\text{cm}^{-1}$ . Figure 3 shows the transmission spectra as a function of wavenumber for PZT powders heated at different temperatures. In this wavenumbers interval, a broad band was observed for each spectrum from 850 to 590  $\text{cm}^{-1}$  with a maximum absorbance in the vicinities of 547  $\text{cm}^{-1}$ . This peak has been associated with the vibration of M–O (M = metal) bonds in the systems.<sup>15</sup> There are some other peaks in the range of 1400–2400  $\text{cm}^{-1}$  belongs to vibrations of  $-\text{CNO}_2$ ,  $-\text{COO}$  and  $\text{C-O}$ ,  $\text{C=O}$ .<sup>16</sup> These peaks of organic materials start to disappear as the calcinated temperatures increase.

The band in the vicinities of 547  $\text{cm}^{-1}$  is associated to  $\text{BO}_6$  octahedron bond and indicates the formation of a perovskite phase starts to take

Table 1. Lattice parameters of PZT (95/5) nanopowders calcinated at different temperatures.

| Temperatures (°C) | $2\theta$ (degree) | ( $hkl$ ) | Phase        | Lattice parameters (Å°)           | Volume (Å°) <sup>3</sup> |
|-------------------|--------------------|-----------|--------------|-----------------------------------|--------------------------|
| 600               | 30.34              | 110       | Orthorhombic | $a = 5.506, b = 5.610, c = 5.700$ | 176.065                  |
| 700               | 30.21              | 110       | Orthorhombic | $a = 5.512, b = 5.703, c = 5.751$ | 180.782                  |
| 800               | 30.115             | 110       | Orthorhombic | $a = 5.760, b = 5.930, c = 5.825$ | 198.964                  |

Table 2. Mean particles size of samples calcinated at different temperatures.

|                  | Temperatures<br>(°C) | Mean particles<br>size (nm) |
|------------------|----------------------|-----------------------------|
| <u>This work</u> |                      |                             |
| PZT (95/5)       | 500                  | 12.0                        |
|                  | 600                  | 40.33                       |
|                  | 700                  | 40.33                       |
|                  | 800                  | 42.44                       |
| <u>Others</u>    |                      |                             |
| PZT (95/5) [14]  | 500–550              | 30–70                       |
| PZT (53/47) [15] | 500                  | 36.0                        |
|                  | 550                  | 48.0                        |
|                  | 600                  | 61.0                        |
|                  | 650                  | 78.0                        |

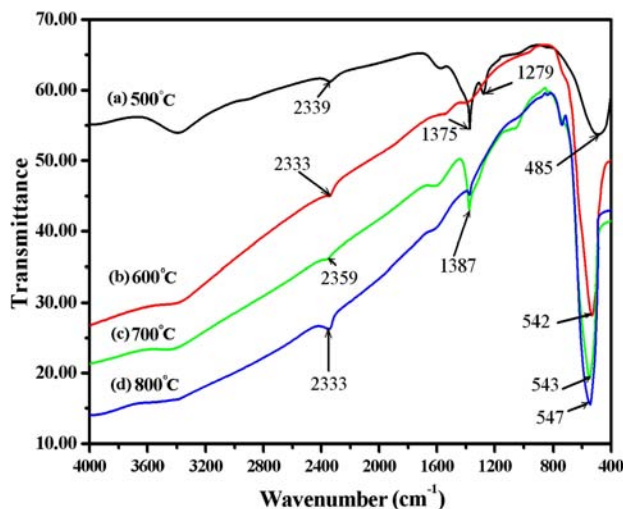


Fig. 3. FTIR spectra of PZT nanopowders treated at different temperatures. (a) 500°C, (b) 600°C, (c) 700°C and (d) 800°C.

place for all calcinated temperatures and starts to increase in proportion with the temperature.<sup>17</sup> This result is consistent with the other data that prepared PZT in different routes such as the polymeric citrate precursor.<sup>18</sup> Bands associated with Pb ions were not observed in the mid-infrared spectra because of their heavy mass.

### 3.3. Evaluation of the optical constants

We used Kramers–Kronig analysis to evaluate the optical constants of PZT (95/5) powders prepared by gel-combustion method using FTIR spectra data.<sup>19</sup> The IR spectra (Fig. 3) show the absorbance values are less than 67%. As a result, the absorption coefficient ( $A$ ), in the strong absorption region

where the envelop method is not valid, should be evaluated from the optical transmittance data using Lambert's principle<sup>20</sup>:

$$A = - \left( \frac{1}{t} \right) \ln T \quad (1)$$

where  $T$  is the transmittance and  $t$  is the thickness of the KBr pellet prepared for IR measurements. Knowing both  $t$  and  $T$ , we may calculate the absorption coefficient from Eq. (1). Then, the experimental values of reflectance spectra of nanopowder PZT can be evaluated from FTIR transmittance and Eq. (1) as follows:

$$R + T + A = 1 \quad (2)$$

where  $R$  is the reflectance coefficient and  $A$  is the absorbance coefficient. The complex refractive index can be calculated from the following equation<sup>21</sup>:

$$\tilde{n}(\omega) = n(\omega) + ik(\omega) \quad (3)$$

where  $n$  is the real and  $k$  is the imaginary parts of complex refractive index. Knowing the values of reflectance,  $R(\omega)$ , in all frequencies, the refractive index and the extinction coefficient can be calculated from the following relations:

$$n(\omega) = \frac{1 - R(\omega)}{1 + R(\omega) - 2 \cos \varphi(\omega) \sqrt{R(\omega)}} \quad (4)$$

$$k(\omega) = \frac{2 \sin \varphi(\omega) \sqrt{R(\omega)}}{1 + R(\omega) - 2 \cos \varphi(\omega) \sqrt{R(\omega)}} \quad (5)$$

The phase of reflectance wave,  $\varphi(\omega)$ , can be obtained by Kramers–Kronig's dispersion:

$$\varphi(\omega) = - \frac{\omega}{\pi} \int_0^{\infty} \frac{\ln R(\omega') - \ln R(\omega)}{\omega'^2 - \omega^2} d\omega' \quad (6)$$

For calculating  $\phi(\omega)$  several extrapolation approaches have been evaluated and reported.<sup>22,23</sup> We have calculated  $\phi(\omega)$  by Maclaurin's method<sup>24</sup> from Eq. (7), this method is rather accurate, but it needs double Fourier transform and the calculation takes a relatively longer time.

$$\varphi(\omega_g) = \frac{2\omega_g}{\pi} \times 2h \times \sum_i \frac{\ln(\sqrt{R(\omega)})}{\omega_i^2 - \omega_g^2}. \quad (7)$$

where  $h = \omega_{i+1} - \omega_i$  and if data interval  $g$  is an odd number then  $i = 2, 4, 6, \dots, g-1, g+1, \dots$ , while if  $g$  is an even number then  $i = 1, 3, 5, \dots, g-1, g+1, \dots$ .

The reflectance ( $R$ ) and the phase transition ( $\varphi$ ) spectrum in the range of 400–1200  $\text{cm}^{-1}$  for

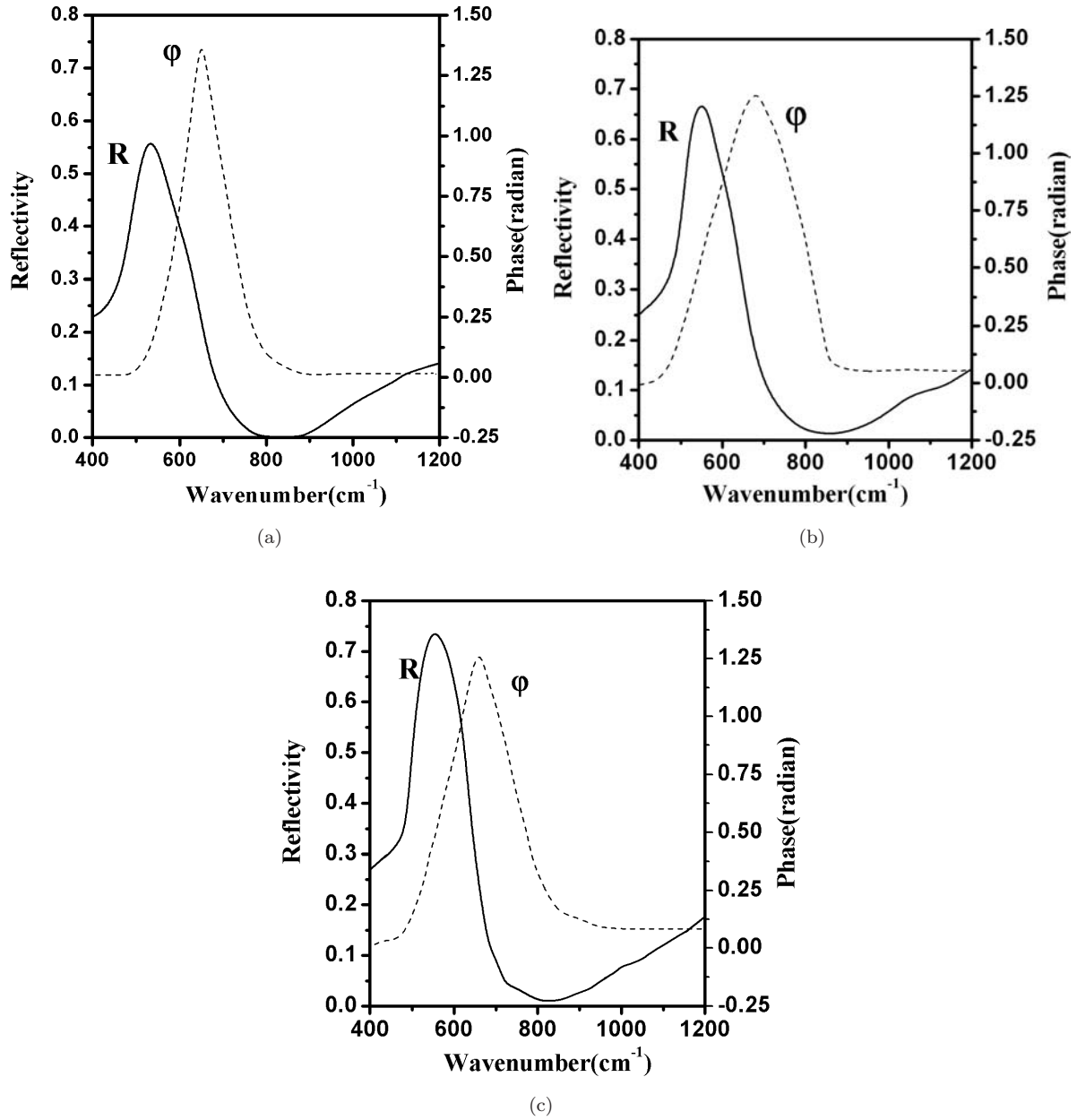


Fig. 4. Reflectance and the phase change spectrum of PZT nanopowders calcinated at different temperatures (a) 600°C, (b) 700°C and (c) 800°C.

PZT nanopowders calcinated at different temperatures are shown in Fig. 4. The values of  $R$  and  $\varphi$  change as the temperature increase and the peak value of  $R$  is shifted to higher wavenumber.

Figure 5 shows the refractive index and extinction coefficient from 400  $\text{cm}^{-1}$  to 1200  $\text{cm}^{-1}$  for PZT nanopowders calcinated at different temperatures. The values of refractive index are not constant and vary as temperature changes. The strong decrease in the refractive index is associated with the fundamental band gap absorption. Increasing calcinated

temperature shifts the peak values of  $n$  towards larger wavenumber.

Assuming the infrared radiation is incident normal to the surface of the sample and knowing the values of  $n$  and  $k$ , the real ( $\epsilon'$ ) and imaginary ( $\epsilon''$ ) parts of the complex dielectric function ( $\tilde{\epsilon}(\omega) = \epsilon'(\omega) + i\epsilon''(\omega)$ ) can be calculated using the relations<sup>25,26</sup>:

$$\epsilon'(\omega) = n^2(\omega) - k^2(\omega) \quad (8)$$

$$\epsilon''(\omega) = 2n(\omega)k(\omega) \quad (9)$$

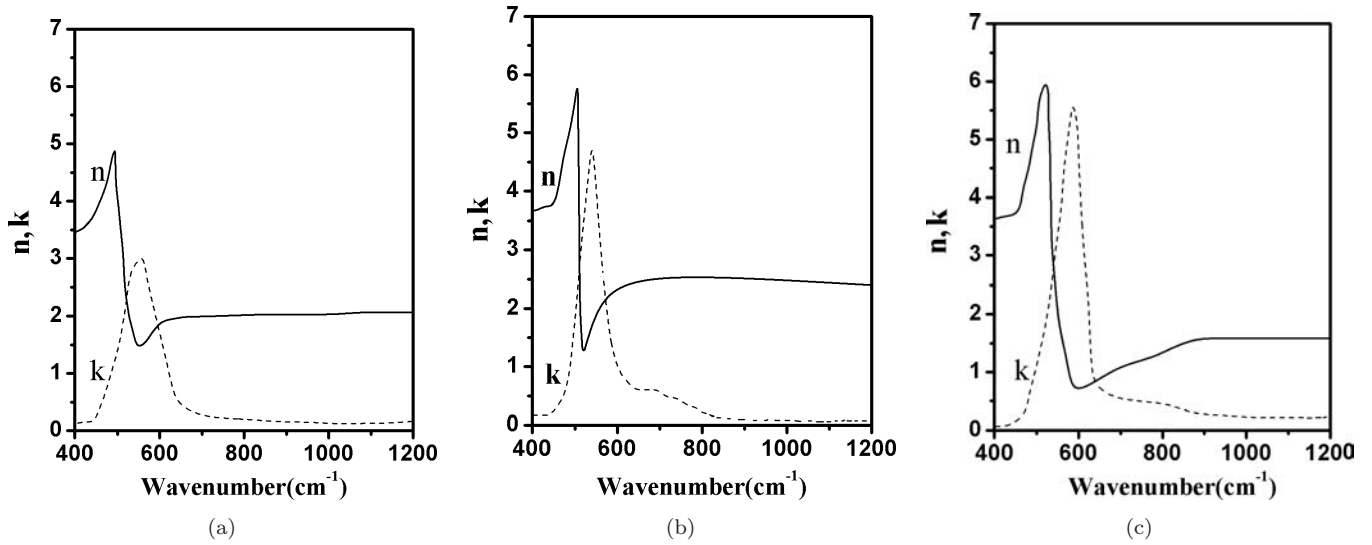


Fig. 5. Refractive index and extinction coefficient of PZT nanopowders calcinated at different temperatures (a) 600°C, (b) 700°C and (c) 800°C.

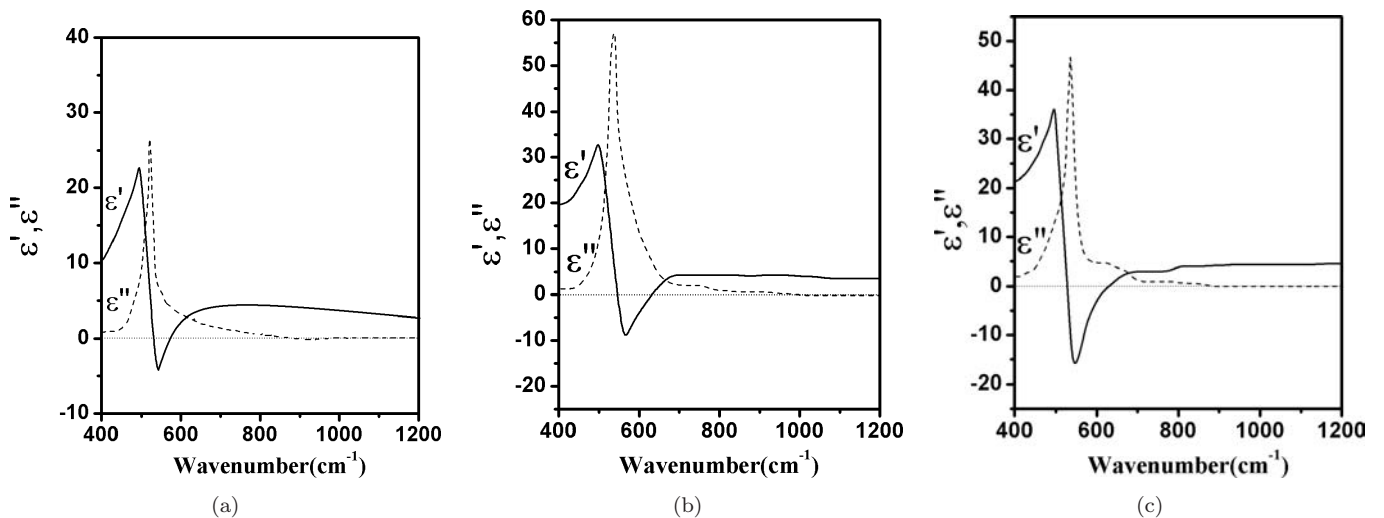


Fig. 6. Real and the imaginary parts of dielectric function for PZT nanopowders calcinated at different temperatures (a) 600°C, (b) 700°C and (c) 800°C.

The real and the imaginary parts of the frequency dependent dielectric function for the PZT (95/5) nanopowders calcinated at different temperatures are shown in Fig. 6.

The curves are flat in the long-wavenumber region and rises rapidly at 606  $\text{cm}^{-1}$ . The real and imaginary parts of dielectric function are increased slowly with increasing temperatures as the structure changes with the temperature.

When the value of real dielectric function is negative around 650  $\text{cm}^{-1}$  in Fig. 6, the reflection is maximum. The incident energy is starting to absorb by the material from onset of region when

the real part of dielectric function approaching is zero and thus the reflection goes to zero. This of course happens at plasmon frequency, i.e., the frequency of collective oscillations of the valence electrons.

In IR spectrum study, the optical phonons (LO and TO) are the frequencies of interest for describing the optical interactions with the lattice. In general, these interactions will lead to a characteristic optical, i.e., the sharp increase of reflectance caused by the resonance of transverse optical phonon (TO) and the decrease at the resonance of the longitudinal optical phonon (LO).

Table 3. IR spectra of optical phonon for PZT (95/5) powders treated at different temperatures.

| Temperature (°C)                                | 600 | 700 | 800 |
|---|-----|-----|-----|
| Transverse optical phonon (TO) $\text{cm}^{-1}$ | 525 | 530 | 541 |

From the above discussion, once the phase  $\varphi(\omega)$  value is obtained, the optical and dielectric constants can be determined from numerical calculation. Consequently, the TO and LO mode can be easily determined from the maximum position of  $\varepsilon''$  and from the peak position of  $\text{Im}(-1/\varepsilon)$  curves, respectively.

The transverse optical phonon frequency determined from the maximum position of imaginary dielectric function for PZT powder at different temperatures are presented in Table 3.

#### 4. Conclusions

The pyroelectric nanopowders base on PZT (95/5) has been synthesized by the sol-gel method using citric acid as complexing reagent. The XRD patterns and FTIR spectra indicate the perovskite phase started to form at calcination temperature of 600°C together with the pyrochlore phase. As the temperature increased the perovskite start to increase in portion, but the pyrochlore phase disappeared at a temperature of 800°C. The results calculated from Scherrer formula show that as the calcinations temperature increased, the particle size was also increased.

The IR spectra show that the absorbance values are less than 67%. As a result, the absorption coefficient ( $A$ ) was evaluated from the optical transmittance data using Lambert's principle. We used Kramers-Kronig analysis to evaluate the optical constants of PZT powders using FTIR spectra data. The optical properties of the pyroelectric nanopowders have been investigated in the wavenumber range of 400–4000  $\text{cm}^{-1}$ . The optical constants of nanopowder are changing with calcinated temperatures. It seems that the most obvious reason for the change of optical constant is due to change of structural parameters.

#### Acknowledgments

The Ferdowsi University of Mashhad (Iran) as a grant project supports this work. The authors are grateful to Dr. Tayari (Department of Chemistry Ferdowsi University of Mashhad) for his technical assistance in recording FTIR spectrum.

#### References

1. M. Schreiter, R. Gabl, J. Lerchner, C. Hohlfeld, A. Delan, G. Wolf, A. Blüher, B. Katzschner, M. Mertig and W. Pompe, *Sensors Actuators B: Chem.* **119**, 255 (2006).
2. P. Guggilla, A. K. Batra, J. R. Currie, M. D. Aggarwa, M. A. Alim and R. B. Lal, *Mater. Lett.* **60**, 1937 (2006).
3. W. Chaisan, R. Yimnirun, S. Ananta and D. P. Cann, *Mater. Lett.* **59**, 3732 (2005).
4. N. Okada, K. Ishikawa, K. Murakami, T. Nomura, M. Hagino, N. Nishino and U. Kihara, *Jpn. J. Appl. Phys.* **31**, 3041 (1992).
5. A. C. Tas and B. A. Tuttle, *J. Am. Ceram. Soc.* **82**, 1582 (1999).
6. B. W. Lee, *J. Eur. Ceram. Soc.* **24**, 925 (2004).
7. Y. Deng, L. Liu, Y. Cheng, C. W. Nan and S. J. Zhao, *Mater. Lett.* **57**, 1675 (2003).
8. J. Y. Choi, C. H. Kim and D. K. Kim, *J. Am. Ceram. Soc.* **81**, 1353 (2005).
9. N. Chakrabarti and H. S. Maiti, *Mater. Lett.* **30**, 169 (1997).
10. M. Cernea, G. Montanari, C. Galassi and A. L. Costa, *Nanotechnology* **17**, 1731 (2006).
11. G. Montanari, A. L. Costa, S. Albonetti and C. Galassi, *J. Sol-Gel Sci. Technol.* **36**, 203 (2005).
12. L. Jiankang and Y. Xi, *J. Wuhan University Technol. Mater. Sci. Ed.* **20**, 26 (2005).
13. G. Mu, S. Yang, J. Li and M. Gu, *J. Mater. Process. Technol.* **182**, 382 (2007).
14. S. Linardos, Q. Zhang and J. R. Alcock, *J. Eur. Ceramic Soc* **26**, 117 (2006).
15. C. H. Perry, B. N. Khanna and G. Rupprecht, *Phys. Rev.* **135**, A408 (1964).
16. K. Nakamoto, *Infrared and Raman Spectra of Inorganic and Coordination Compounds* (John Wiley & Sons, 1997).
17. Y. Yoshikawa and K. Tsuzuki, *J. Am. Ceram. Soc.* **75**, 2520 (1992).
18. P. Jha, P. R. Arya and A. K. Ganguli, *Mater. Chem. Phys.* **82** 355 (2003).
19. C. A. Sergides, A. R. Chughtai and D. M. Smith, *Appl. Spectrosc.* **41**, 154 (1987).
20. P. Prathap, Y. P. V. Subbaiah, M. Devika and K. T. Ramakrishna Reddy, *Mater. Chem. Phys.* **100**, 375 (2006).
21. F. Stern, *Solid State Phys.* **15**, 327 (1963).
22. D. M. Roessler, *Br. J. Appl. Phys.* **17**, 1313 (1966).
23. D. M. Roessler, *Br. J. Appl. Phys.* **16**, 1119 (1965).
24. M. Abramowitz and I. A. Stegun, *Handbook of Mathematical Functions* (Dover, New York, 1965).
25. J. C. Manificier, J. Gasiot and J. P. Fillard, *J. Phys E: Sci. Instrum.* **9**, 1002 (1976).
26. S. B. Majumder, Y. N. Mohapatra and D. C. Agrawal, *J. Mater. Sci.* **32**, 2141 (1997).